Optik 127 (2016) 1078–1083

Contents lists available at ScienceDirect

Optik

journal homepage: www.elsevier.de/ijleo

Numerical simulation and experiments of ground-based laser irradiating small scale space debris

Yingwu Fang*, Liwei Yang, Shanghong Zhao, Yi Wang

Information and Navigation College, Air Force Engineering University, Xi'an 710077, PR China

ARTICLE INFO

Article history:
Received 19 January 2015
Accepted 26 October 2015

Keywords:
Ground-based laser
Space debris
Laser irradiation
Dynamic model

ABSTRACT

This article investigated the effects of ground-based laser irradiating small scale space debris by numerical simulation and experiments. A dynamic model of ground-based laser irradiating small scale space debris was established, and the waveforms and arriving position of shock wave propagation with different laser pulses width were analyzed, the interaction relationship of jet velocity with different laser energies was discussed, and the distributed rules of impulse coupling coefficient with different laser pulses width and power densities were also described. As a result, the removing effect of the small scale debris was described to evaluate the cleaning influence. This paper provides analyses for establishing removing schemes of small scale debris and selecting suitable parameters ground-based laser system.

1. Introduction

There are a lot of small-sized bodies by space activity since October 1957, such as space debris and space dusts. Especially, the space debris is artificially originated fragments upon rockets launch, etc. By the year 2014, there were about 670 thousand space debris with dimension of about 1–10 cm or more according to NASA [1–3]. It is rather difficult to monitor the space debris with small dimension of 1–10 cm level by conventional means. Hence, these centimeter-scale debris are called small scale space debris. At present, the amount of small scale space debris is increasing due to the increase of space activities in low-earth orbits [4]. The small scale space debris is one of the most dangerous environment factors to spacecraft because their velocities are 10 km/s or so, they are threatening the security of the orbiting space vehicles, and the impact damage will result in degradation and/or failure of space materials, leading to the decrease of stability and life of spacecraft [5,6]. Hence, research the removing technology of small scale space debris is very important to safely develop and utilize space resource for long.

A commonly used technique for removing small scale space debris is multi-pulse laser irradiation technology, and it is regarded as a feasible approach to clean scale space debris, and the clean core is that space debris obtains reversed velocity increment to realize orbit maneuver by laser irradiation. Sakai et al. analyzed the interaction mechanism of laser with target and vaporized target material, and discussed impulse generation on aluminum target irradiated with Nd: YAG laser pulse in ambient gas [7]. Sinko et al. presented a alternate model to address CO_2 laser ablation impulse of polymers in vapor and plasma regimes [8]. Phipps et al. presented an orion plan to remove space debris by using a 20 kW, 530 nm, pulse laser, and discussed the feasibility for laser removing space debris. Furthermore, Phipps et al. given an analytical model for calculating laser ablation impulse coupling coefficient, and discussed an alternate treatment of the vapor–plasma transition [9,10]. Lee et al. investigated the measurement method of freely-expanding plasma from hypervelocity space debris and space vehicle impacts [11], and Schall discussed the feasibility and basic principle for cleaning space debris from lower earth orbits by laser radiation [4]. An given a velocity model for predicting debris clouds produced by hypervelocity impacts in space by the two-stage light-gas gun impacting 6061-T6 aluminum sheets [12]. Jin et al. analyzed removal method of elliptic orbit space debris using ground-based laser, and the simulation results showed that the high power pulse laser can be considered as a feasible method to clean space debris [13]. In general, most researches have shown that high power pulse laser can clean space debris efficiently, but little attention has been focused on the discussion removal effects for laser irradiation small scale space debris. Hence, further studies on the effects of laser irradiating small scale space debris with different laser parameters are very important.

At present, no matter using space based or ground based (including air based) laser irradiating method, neither of them has absolute advantage to remove small scale space debris. Especially, the action mechanism of high power laser removing small scale space debris still lacks of understanding further. Hence, the aim of this article

* Corresponding author. Tel.: +86 13659206026.
E-mail address: yiwangfang88@163.com (Y. Fang).

http://dx.doi.org/10.1016/j.ijleo.2015.10.142
0030-4026/

is to discuss the effects of ground-based laser irradiating small scale space debris with different laser parameters by numerical simulations and experiments, and it has very important theoretical significance and practical value for selecting suitable ground-based laser parameters and efficient removal schemes.

2. Analysis of removing method

According to the NASA's ground experiments of high speed collision disaggregation on satellites, space debris have various shapes, in which debris with the shape of flake, block, rod and irregular shape take up most of the debris. There are three main space debris removal methods proposed in and abroad, namely tethered dragging, trapping and laser irradiating. Based on the existing technology, laser irradiation technology is the most promising method to remove space debris, and it is the emphasis of current researches. At present, the main removal method of space debris includes based-space system and based-ground system by laser irradiation.

Based-space laser monitoring and removing system is closer to the debris, and the problems of atmosphere transmission and control is no longer serious. However, the cost to launch the laser monitoring and removing system to LEO is about $20/g based on the NASA, and the problems of based-space debugging, replenishment are also complex, which would cost more than 2 times than developing based-ground system [14,15]. In addition, power density of continuous wave lasers irradiated on debris can hardly reach the breakdown threshold. Under this condition, space debris will be melted into more small parts and the target of removing cannot be effectively achieved. Therefore, various of countries pay attention to based-ground pulse laser monitoring and removing technologies, the most noted research is the Orion plan supported by NASA and USAF. Solid laser with pulse width of 10 ns is well developed in 1990s, hence Orion system choose based-ground Nd: lasers with average power of 30 kW (pulse width 10 ns) as a laser source. Accurate position of space debris is first monitored and detected by laser, and then high power laser is irradiated to the surface of space debris (power density larger than breakdown threshold) through tracing and aiming transmitter and self-adaption optical system. Space debris with small size can be totally ablated. For space debris with large size, during the process of laser impulse coupling, the debris can obtain a speed increment, and the debris will fall into aerosphere and burn off when the increment meets a certain condition [16,17]. Namely, the irradiated debris can be captured by atmosphere when the debris enter into the critical orbit altitude of 200 km or so. Finally, the semi-minor axis height of debris orbit is decreased by decreasing debris orbital speed through laser irradiation. Fig. 1 shows the basic removing principle based on high power laser.

3. Dynamic model of irradiating debris

In order to establish a dynamic model of laser irradiating small scale space debris, assumption conditions are given as follows. The pulse width of ground-based high energy laser is ns-level

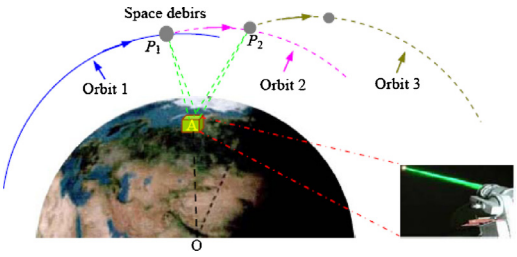

Fig. 1. Basic removing principle based on high power laser.

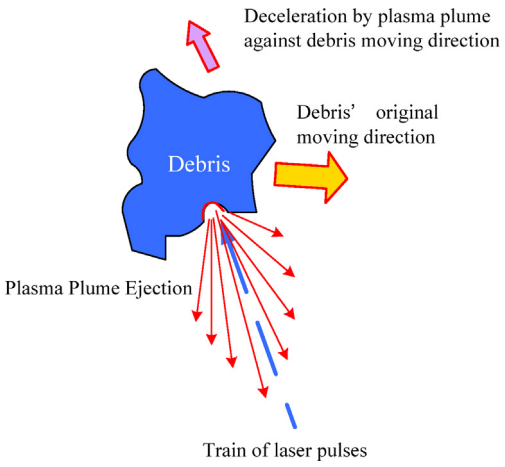

Fig. 2. The sketch map of laser irradiating small scale space debris.

generally. Hence, ground-based laser is assumed to be on the sub-track of space debris [18]. The velocity increment of debris is assumed to gain instantly, and the debris orbit changes are neglected during laser pulse, but the orbit changes in the pulse interval can't be ignored. At the same time, let the shape of space debris be a sphere, the spin of debris be ignored. So, the direction of achieved velocity and laser irradiation is always same. Based on literatures [19], a sketch map of laser irradiating small scale space debris was given, as shown in Fig. 2.

According to Fig. 2, let S be the area of light spot on the target, φ be energy density on the target, ε be transmission coefficient, W be pulse energy, and the following equation is obtained.

$$\phi S = W\varepsilon \tag{1}$$

Assuming S completely fall on the target, then

$$S = \frac{1}{4}\pi d_S^2 \tag{2}$$

Let C_m be impulse coupling coefficient, μ be the rate of debris mass and area, η be velocity change factor, the velocity change of the debris is given by

$$\Delta v = \eta C_m \frac{\phi}{\mu} \tag{3}$$

Substituting Eqs. (1) and (2) in Eq. (3), the velocity increment Δv is expressed as follows

$$\Delta v = \eta C_m \frac{W\varepsilon}{\mu S} = \eta C_m \frac{4W\varepsilon}{\mu\pi {d_S}^2} \tag{4}$$

According to Eq. (4), C_m is target impulse gained from the unit incident laser energy. Impulse coupling coefficient is a parameter that directly relates target impulse to laser energy, and its value reflects the energy utilization in the process of laser ablation in a certain extent. It is influenced by parameters of incident laser, laser energy distribution on the target, and target surface material and target surface structure. The following will discuss the calculating method of C_m.

According to the definition of impulse coupling coefficient, C_m is expressed as follows:

$$C_m = \frac{mv_0}{E_1} = \frac{P}{I} \tag{5}$$

where E_1 is the laser energy, m is the quality of target, v_0 is the achieved target velocity, P is peak pressure on target surface, I is incident laser power density.

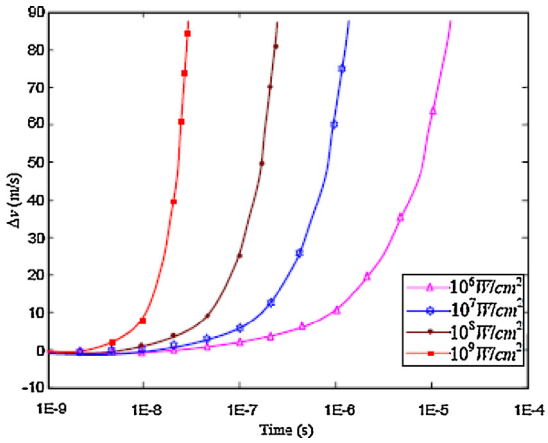

Fig. 3. The curves of velocity increment and action time for different power densities.

Phipps analyzed a number of metal and nonmetal materials [20], and the expression of target surface peak pressure P is given by.

$$P = bI^{n+1}\left(\lambda\sqrt{T}\right)^{n} \tag{6}$$

where b and n are constants, for metal and carbon-hydrogen material, b is approximately equal to 5.6 and 6.5, respectively, while n is −0.3 for different materials, T is laser pulse width, λ is laser wavelength.

The corresponding expression is achieved by combining Eqs. (5) and (6).

$$C_m = bI^{n}\left(\lambda\sqrt{T}\right)^{n} \tag{7}$$

Aluminium alloy belongs to common materials of space debris. In order to establish a calculating model of unified impulse coupling coefficient, the model of laser irradiating aluminium is established.

$$C_m = 5.56\delta\left(I\lambda\sqrt{T}\right)^{-0.301} + P_0(1-\delta)\left(\frac{T-t}{IT}\right) \tag{8}$$

where t is gasification time, P is constant steam pressure, δ is the degree of ionization.

According to Eq. (8), when the laser power density is high enough, the degree of ionization δ is approximately equal to 1, Eq. (8) is represented as follows [21]:

$$C_m = 5.56\left(I\lambda\sqrt{T}\right)^{-0.301} \tag{9}$$

As a result, velocity increment Δv is calculated by substituting Eqs. (7) and (9) into Eq. (4). Related studies show that different scaling relations results can produce different surface pressure values. These values are not very accurate, but they have almost same order of magnitude. At the same time, different scaling relations may lead to different impulse coupling coefficient values if the target surface is obtained by using the empirical relationship. Generally, impulse coupling coefficient value is 1×10^{-5}–10×10^{-5} N s/J.

Table 1
Basic laser parameters during effective work time (Δv = 20 m/s).

Power density on target (W/cm^2)	Transmitting power (W)	Pulse width (μs)	Effective time (μs)	Pulse
10^6	2×10^{10}	10^0	3.0	3
10^7	2×10^{11}	10^{-1}	0.5	4
10^8	2×10^{12}	10^{-2}	0.08	8
10^9	2×10^{13}	10^{-3}	0.01	10

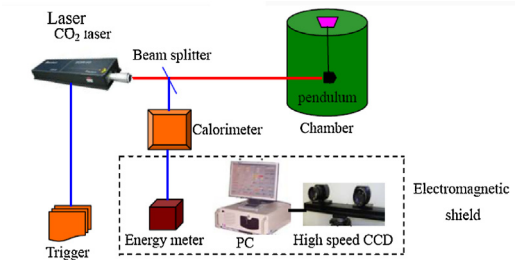

Fig. 5. The experimental framework of impulse coupling coefficient.

Further, in order to analyse the propagation characteristics of laser induced shock waves, a fluid dynamics method is used for modeling and describing the propagation process of laser induced shock wave. According to ideal fluid elastoplastic model, the Lagrangian equations for one dimensional plane flow are given as follows:

$$\begin{cases} u = \dfrac{\partial U}{\partial t};\ v = \dfrac{1}{\rho}\dfrac{\partial U}{\partial w} \\ \dfrac{\partial u}{\partial t} + \dfrac{1}{\rho}\dfrac{\partial(\sigma+q)}{\partial w} = 0;\ \dfrac{\partial E}{\partial t} + (\sigma+q)\dfrac{\partial v}{\partial t} = 0;\ \sigma = P + S \\ \dfrac{\partial S_d}{\partial t} = 2G\left(\dfrac{1}{3v}\dfrac{\partial v}{\partial t} - \dfrac{\partial u}{\partial U}\right);\ \left|S_d\right| < \dfrac{2}{3}Q \\ S_d = \pm\dfrac{2}{3}Q;\ \left|S_d\right| \geq \dfrac{2}{3}Q \end{cases} \tag{10}$$

where U is Euler coordinate, w is Laplace coordinate, u is particle velocity, ρ is normal density, v is specific volume, σ is stress, q is artificial viscosity, E is internal energy, S_d is deviatoric stress, G is shear modulus, Q is yield strength.

At last, a corresponding state equation is established as follows:

$$P = P(E, v) \tag{11}$$

According to the above equation, the finite difference method is used to design the corresponding dynamic response analysis program. Finally, the propagation process of laser induced shock waves can be made.

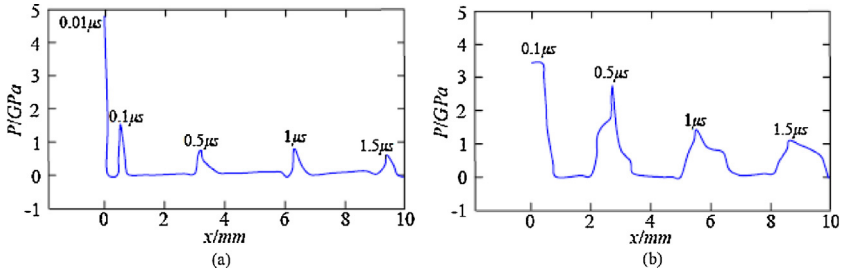

Fig. 4. The waveforms and arriving position of shock wave with different laser pulse width. (a) 0.01 μs; (b) 0.1 μs.

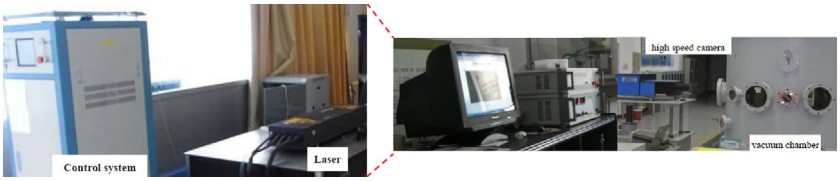

Fig. 6. The main experimental facility and part scene.

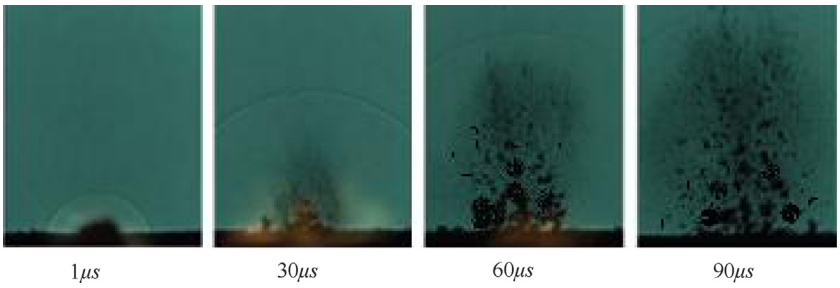

Fig. 7. The results of plasma plume expansion at different times within 100 ns.

4. Results and analysis

Commonly, aluminium alloy materials are one of the main elements for space debris. As an example, the relation between speed increment and different power density was discussed using the typical aluminium alloy materials. Because small scale space debris is mainly distributed at the altitudes of 800–1200 km, so the altitude of 1000 km was chosen in this example. Let the mass of small scale space debris was 80 g, the debris size was 10 cm × 10 cm, the thickness was 1 mm, the laser wavelength was 532 nm, the power density was 10^6–10^9 W/cm^2, the laser pulse width was 1 ns–1 ms. Finally, the relationship of velocity increment and action time was obtained by laser irradiating debris. Fig. 3 showed the curves of velocity increment and action time for different power densities.

According to Fig. 3, it was seen that the velocity increments were increased with the increase of power density. Based on the mechanism of laser removing space debris, pulse lasers which provide power density of 10^6–10^9 W/cm^2 on target can be used to remove space debris, so there are many choices of laser source required for removing space debris. For example, when $\Delta v = 20$ m/s, the effective laser work time required for corresponding typical power density was obtained by numerical simulation, as shown in Table 1.

The following discussed the influence rules of different laser pulses width on shock wave propagation and impulse coupling coefficient in detail. Two kinds of propagation process of laser shock wave were simulated. Laser wavelength was 1.06 μm, irradiation pulse width was 10^{-8} s, power density was 10^8 W/cm^2, and peak pressure on the surface of the aluminum target was 4.85 GPa. As

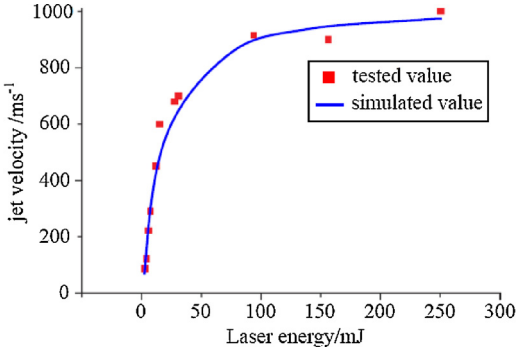

Fig. 8. The relational curve of jet velocity with different laser energy.

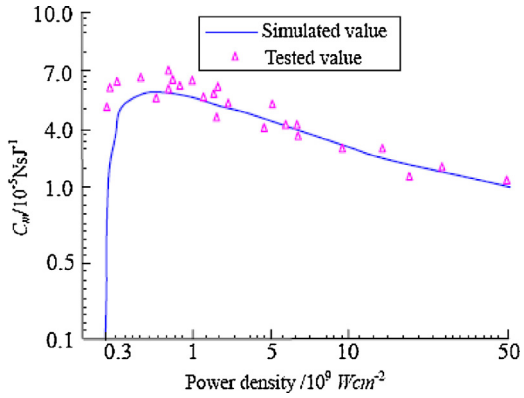

Fig. 9. The relational curve of impulse coupling coefficient with different power density.

a result, the waveforms and arriving position of shock wave was obtained with different laser pulses by numerical simulation, as shown in Fig. 4(a). At the same time, the laser power density was kept unchanged, the pulse width was adjusted to 10^{-7} s, the surface peak pressure was 3.66 GPa. Finally, the waveforms and arriving position of shock wave were also obtained, as shown in Fig. 4(b). It can be seen in Fig. 4(a) that the shock wave was attenuated rapidly, it was faded down the elastic wave after about 0.5 μs, and the peak

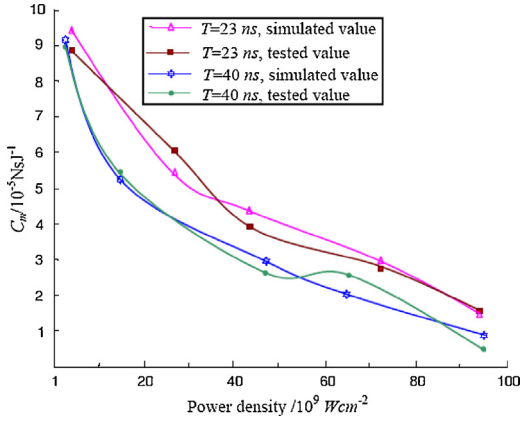

Fig. 10. The distribution curve of impulse coupling coefficient with power density.

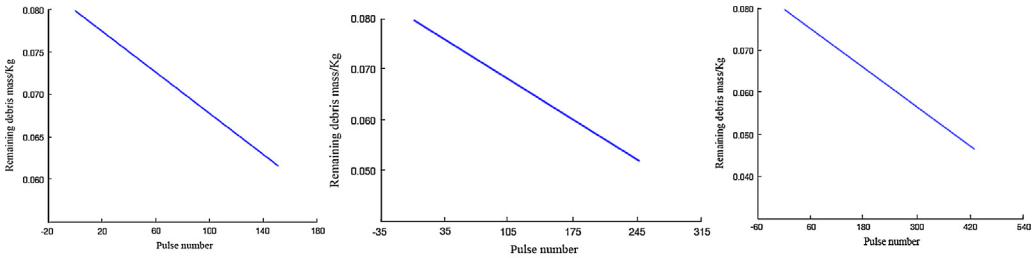

(a) 800 *km* (b) 1000 *km* (c) 1200 *km*

Fig. 11. The cleaning effect of removing space debris.

pressure was about 0.52 GPa. By Comparing with Fig. 4(a) and (b), the results shown that the surface peak pressure was decreased 1.23 GPa, but the attenuation of shock wave was much slower, and the shock wave had obvious broadening. Hence, the difference of laser pulses width has great effect for shock wave propagation on the target.

Second, the relationship of aluminum impulse coupling coefficient and laser power density was calculated using Eq. (8). Based on the literatures [22,23], the corresponding experimental method of impulse coupling coefficient was adopted to measure the impulse coupling coefficient. Experimental devices are mainly composed of laser, loading beam splitter, pendulum, energy meter and high speed CCD, etc. The experimental framework of impulse coupling coefficient was shown in Fig. 5, and the experimental facility and part scene was shown in Fig. 6.

In order to investigate the plume dynamic property ablated by nanosecond laser ablation, a fast gated intensified CCD camera with a gate width of 3 ns was used to capture the images, and Fig. 7 shown the results of plasma plume expansion at different times within 100 ns. According to the evolution photos of the plume flow field in Fig. 7, the distance of shock propagation along the direction of the incident laser was slightly larger than the other direction. Finally, the shape of wavefront was changed from the semi elliptical sphere to hemisphere in the whole evolution stage.

Further, by adjusting the voltage to control the laser output energy in the experiment, it was found that the jet velocity of plume had great difference for different laser energies when laser irradiating the aluminium alloy materials, and the simulated values and tested results were shown in Fig. 8. The results of numerical calculation and experimental measurement were obtained, and the relational curve of impulse coupling coefficient with power density was shown in Fig. 9.

According to Fig. 8, the simulation results agreed well with the experimental values. Especially, the jet velocity of plume was increased with the increase of the incident laser energy when the laser energy was less than 80 mJ, and the speed was increased significantly. When the laser energy was greater than 80 mJ, the increased speed trend was turned slow for the jet velocity of plume with the increase of laser energy. Finally, the jet velocity tended to a steady value. According to Fig. 9, the pink dots represented tested values by using laser wavelength of 1.06 μm and pulse width of 30 ns, the blue curve represented computed values, and the optimal impulse coupling of aluminum was $(5 \pm 2) \times 10^{-5}$ N s/J. It can be seen that the computed results fit well with the experimental results. In particular, with the increase of laser power density, impulse coupling coefficient was increased first, and it was decreased finally. At the same time, the stage of gasification was undergone firstly, and it was transmitted to plasma subsequently. Owing to the effect of plasma shield, impulse coupling coefficient was reduced gradually, and the optimal impulse coupling could be achieved.

Furthermore, the influence rules of impulse coupling coefficient with different laser pulse width were mainly investigated by numerical simulation and experiment. The laser wavelength was 248 nm, and the distribution curves of impulse coupling coefficient with power density were addressed when the pulse width was 23 ns and 40 ns, respectively, as shown in Fig. 10. It can be seen from Fig. 10 that the impulse coupling coefficient was decreased with the increase of laser power density when the laser wavelength was definite. Especially, the impulse coupling coefficient was obviously increased with decrease of the pulse width. The main cause was that plasma produced could shield subsequent laser, and the short pulse could obtain bigger impulse coupling coefficient.

By simulation and experiments, the relation of velocity increments and impulse coupling coefficient with different laser power density and pulse width have been addressed. Hence, the orbit status of small scale space debris and removing effect can be analyzed according to the above discussion. Owing to the effect of all kinds of linear and nonlinear factor when transmitting high-energy laser by atmosphere, the energy has bad attenuation when the zenith angle is greater than 45°. In this case, let the initial zenith angle was 45°, the velocity increment was 20 m/s. When the altitudes were 800 km, 1000 km and 1200 km, the cleaning effect of removing space debris was obtained by numerical simulation, and the affected curves of pulse number with remaining debris mass at altitudes of 800 km, 1000 km and 1200 km were simulated, respectively, as shown in Fig. 11.

According to Fig. 11, in order to remove small scale space debris effectively, the pulse number of laser must be increased with the increase of altitude. At the altitudes of 800 km, 1000 km and 1200 km, the remaining debris mass was obviously decreased with the increase of pulse number. But it was very difficult for using ns laser to clean small scale space debris by one pass, and multiple passes should be adopted to remove the debris. Especially, at the altitudes of 800 km, 1000 km and 1200 km, the pulse number of 142, 245 and 423 were produced to irradiate the debris. The remaining debris mass were about 0.062 kg, 0.052 kg and 0.047 kg, and perigee altitude of the debris orbit were fallen down gradually. With the increase of orbit, the remaining debris mass was decreased. Finally, the debris orbit was less than 200 km, the debris entered the critical height of aerosphere burnout to be captured. As a result, the debris was removed effectively by laser irradiating process.

5. Conclusions

A ground-based laser system is proved to be an efficient method to clean small scale space debris that poses a threat to a space station. This paper focused on influence rules analysis of ground-based laser irradiating small scale space debris by the simulations and experiments, and the following conclusions were drawn:

(1) A reversed impulse could be generated on Al materials surface, and the surface peak pressure was decreased 1.23 GPa. But the attenuation of shock wave was much slower, and the shock wave has been broadened obviously. The jet velocity of plume was increased with the increase of the incident laser energy

when the laser energy was less than 80 mJ by comparing the calculated results with the experimental values, and the jet velocity tended to a steady value 1 km/s.

(2) The relationship of aluminum impulse coupling coefficient and laser power density was analyzed, and the optimal impulse coupling of aluminum was $(5 \pm 2) \times 10^{-5}$ N s/J. With the increasing of laser power density, impulse coupling coefficient was increased first, and was decreased finally. The impulse coupling coefficient was obviously increased with decrease of the pulse width.

(3) Multiple passes could be adopted to remove the centimeter-scale debris in LEO. The remaining debris mass was obviously decreased with the increasing of the number of laser pulses at the altitudes of 800 km, 1000 km and 1200 km, and the remaining debris mass was also decreased with the increasing of orbit by the numerical simulations. A robust cleaning effect of removing space debris effect was influenced by different orbit elements, impulse coupling coefficient and laser parameters, etc.

Acknowledgements

The authors are grateful for the support provided by the Science and Technology Plan Project of Shaanxi Province, China (grant no. 2013K07-17), the Natural Science Foundation of Shaanxi Province, China (grant no. 2012JM8004), and the National Natural Science Foundation of China (grant no. 61205002).

References

[1] J.C. Liou, N.L. Johnson, N.M. Hill, Controlling the growth of future LEO debris populations with active debris removal, Acta Astronaut. 66 (5) (2010) 648–653.
[2] U.S. Space Surveillance Network, Monthly number of objects in earth orbit by object type, Orbital Debris Q. News 18 (1) (2014) 3–6, ⟨http://www.orbitaldebris.jsc.nasa.gov⟩.
[3] W. Bauer, O. Romberg, A. Pissarskoi, C. Wiedemann, P. Vörsmann, In orbit debris-detection based on solar panels, CEAS Space J. (5) (2013) 49–56.
[4] W. Schall, Laser radiation for cleaning space debris from lower earth orbits, J. Spacecraft Rockets 39 (1) (2002) 81–91.
[5] Z.Z. Gong, K.B. Xu, Y.Q. Mu, Y. Cao, The space debris environment and the active debris removal techniques, Spacecraft Environ. Eng. 31 (2) (2014) 129–135.
[6] C.R. Phipps, J.R. Luke, T. Lippert, M. Hauer, A. Wokaun, Micropropulsion using laser ablation, Appl. Phys. A 79 (4–6) (2004) 1385–1389.
[7] T. Sakai, Impulse generation on aluminum target irradiated with Nd: YAG laser pulse in ambient gas, J. Propul. Power 25 (2) (2009) 406–414.
[8] J.E. Sinko, C.R. Phipps, Modeling CO_2 laser ablation impulse of polymers in vapor and plasma regimes, Appl. Phys. Lett. 95 (13) (2009) 1–3.
[9] C.R. Phipps, G. Albrecht, H. Friedman, D. Gavel, E.V. George, J. Murray, C. Ho, W. Priedhorsky, M.M. Michaelis, J.P. Reilly, Orion: clearing near-earth space debris using a 20 kW, 530 nm, earth-based, repetitively pulse laser, Laser Part. Beams 14 (1) (1996) 1–44.
[10] C.R. Phipps, An alternate treatment of the vapor–plasma transition, Int. J. Aerosp. Innov. 3 (1) (2011) 45–50.
[11] N. Lee, S. Close, D. Lauben, I. Linscott, A. Goel, T. Johnson, J. Yee, A. Fletcher, R. Srama, S. Bugiel, A. Mocker, P. Colestock, S. Green, Measurements of freely-expanding plasma from hypervelocity impacts, Int. J. Impact Eng. 44 (2012) 40–49.
[12] An Kai, A model of velocity for predicting debris clouds produced by hypervelocity impacts in space, Spacecraft Environ. Eng. 31 (1) (2014) 15–18.
[13] X. Jin, Y.J. Hong, H. Chang, Simulation analysis of removal of elliptic orbit space debris using ground-based laser, Acta Aeronaut. Astronaut. Sin. 34 (9) (2013) 2064–2073.
[14] C.R. Phipps, K.L. Baker, B. Bradford, E.V. George, Removing orbital debris with lasers, Adv. Space Res. 49 (2012) 1283–1300.
[15] V.V. Apollonov, High power lasers for space debris elimination, Chin. Opt. 6 (2) (2013) 188–195.
[16] T.V. Bordovitsyna, A.G. Aleksandrova, Numerical modeling of the formation: orbital evolution, and distribution of fragments of space debris in near-earth space, Sol. Syst. Res. 44 (3) (2010) 238–251.
[17] C. Bonnal, J. Ruault, M. Desjean, Active debris removal: recent progress and current trends, Acta Astronaut. 85 (2013) 51–60.
[18] X.L. Xu, Y.Q. Xiong, A research on the collision probability calculation of space debris for nonlinear relative motions, Chin. J. Astron. Astrophys. 35 (3) (2011) 304–317.
[19] Y.V. Afanasiev, O.N. Krokhin, G.V. Sklizkov, Evaporation and heating of a substance due to laser radiation, IEEE J. Quantum Electron. 2 (9) (1996) 483–486.
[20] C. Phipps, M. Birkan, W.L. Bohn, Review: laser ablation propulsion, J. Propul. Power 26 (4) (2010) 609–637.
[21] C. Phipps, T.P. Turner, R.F. Harrison, Impulse coupling to targets in vacuum by KrF: HF, and CO_2 single pulse lasers, J. Appl. Phys. 64 (3) (1988) 1083–1096.
[22] R.Q. Tan, J. Lin, J. Hughes, Experimental study of coupling coefficients for propulsion on TEA CO_2 laser, Proc. Second Int. Symp. Beamed Energy Propul. 702 (1) (2004) 122–128.
[23] B. Yang, Y.N. Yang, J.R. Zhu, The experiment study of impulse coupling coefficient under different pressure of ambient air, Optoelectron. Technol. 27 (2) (2007) 92–96.